

Role of the rapid delayed rectifier K⁺ current in human induced pluripotent stem cells derived cardiomyocytes

Makarand Deo¹, Akwasi Akwaboah¹, Bright Tsevi¹, Jacqueline A Treat², Jonathan M Cordeiro^{2*}

¹Department of Engineering, Norfolk State University, Norfolk, Virginia, USA

²Department of Experimental Cardiology, Masonic Medical Research Institute, Utica, New York, USA

*Author for correspondence:
Email: jcordeiro@mmri.edu

Received date: September 30, 2020
Accepted date: November 13, 2020

Copyright: © 2020 Deo M, et al. This is an open-access article distributed under the terms of the Creative Commons Attribution License, which permits unrestricted use, distribution, and reproduction in any medium, provided the original author and source are credited.

Keywords

Electrophysiology, Action potential, Repolarization reserve, Delayed rectifier, Mathematical modeling

The action potential (AP) in cardiac tissue is important for initiating and coordinating contractions in the heart. In addition, the long refractory period minimizes the potential for developing extrasystoles and arrhythmias [1]. The AP is generated by coordinate changes in different ionic currents. In human (or canine) adult ventricular cells, the depolarization phase of the AP is mainly through the influx of Na⁺ and Ca²⁺ through specific voltage gated channels [2]. Repolarization of the AP is regulated by activation of a number of different K⁺ currents which play important roles in regulating the AP. These K⁺ currents include: (i) a Ca²⁺-independent transient outward K⁺ current (I_{to}), (ii) an inwardly rectifying K⁺ current (I_{K1}), and (iii) the rapidly and slowly activating delayed rectifier K⁺ channel currents (I_{Kr} and I_{Ks}, respectively). Previous studies have demonstrated that there is an excess of several K⁺ currents necessary for cardiac repolarization such that a net outward current remains available for repolarization if one or more currents are reduced (repolarization reserve) [3-5]. Therefore, cardiac tissue with a lower repolarization reserve is associated with a prolonged ventricular action potential and an increased incidence of developing arrhythmias [6]. Mutations in KCNH2 (the gene which encodes I_{Kr}) cause a decrease in the magnitude of I_{Kr} and are associated with Long QT syndrome [7,8]. Patients afflicted with Long QT have episodes of fainting, irregular heartbeats and an increased incidence of developing ventricular arrhythmias. Interestingly, many non-cardiac medications have also been shown to block I_{Kr} [9,10] which has resulted in drug companies extensively testing potential therapeutic compounds for I_{Kr} block prior to introduction to the market.

Role of IKr in hiPSC Cardiomyocytes

The importance of I_{Kr} in cardiac repolarization has been highlighted in several studies [11,12]. In recent years, myocytes from large animals are being phased out in favor of human induced pluripotent stem cell derived cardiac myocytes (hiPSC-CM) [13,14]. In contrast to adult myocytes, hiPSC-CMs are deficient or lack several K⁺ currents which are important for repolarization suggesting hiPSC-CMs have a reduced repolarization reserve compared to adult myocytes. These deficiencies include a negligible I_{K1} [15], a functionally absent I_{to} [16] and negligible I_{Ks} [17] suggesting these cells are immature electrophysiologically. The absence of t-tubules coupled with their small size suggests they are morphologically immature [18] indicating that results obtained in hiPSC-CM may not be translatable to the adult phenotype.

There are extensive studies detailing methods to improve the maturity level of hiPSC-CM such as plating hiPSC-CMs on a more rigid matrix [19]. Other investigators have attempted to “mature” hiPSC-CMs by expressing K⁺ current(s) that are not present at this stage of development [20]. In a previous study from our group, we enhanced I_{Kr} by pharmacological methods using several small molecule activators of K⁺ currents (such as NS3623) which have been shown to increase repolarization reserve [21,22]. The results of those studies indicated that I_{Kr} is critical during the repolarization phase of the AP and plays a major role in setting the membrane potential. Inhibition of I_{Kr} (by

Citation: Deo M, Akwaboah A, Tsevi B, Treat JA, Cordeiro JM. Role of the rapid delayed rectifier K⁺ current in human induced pluripotent stem cells derived cardiomyocytes. Arch Stem Cell Ther 2020; 1(1):14-18.

E-4031) resulted in a depolarization of the maximum diastolic potential (MDP) [23]. Conversely, enhancement of I_{Kr} (by NS3623) resulted in a shortening of the hiPSC-CM action potential and hyperpolarization of the MDP [22].

The role of I_{Kr} in modulating the AP duration in hiPSC and native myocytes is well established [24,25]. Tissue type is also important in determining the degree of drug-induced prolongation of the AP, presumably due to the complement of K^+ currents present in the tissue types [4,26]. Figure 1 shows action potentials recorded from hiPSC-CMs and the changes in AP waveform and duration when exposed to low concentrations of the I_{Kr} inhibitor E-4031 (100nM). In response to 100nM E-4031, a triangulation of the AP was observed, and the duration was prolonged (Panels A-B). Prolonged exposure to E-4031 resulted in the development of repolarization alternans (Panel C) and formation of EADs (Panel D).

We next measured the magnitude of I_{Kr} in hiPSC-CMs and the amount of I_{Kr} blockade following 100nM E-4031. Representative traces showing I_{Kr} recorded from hiPSC-CMs in the absence and presence of E-4031 (Figures 2A and 2B). Application of 100nM resulted in a 31% reduction in tail current (Figure 2C). Higher concentrations of E-4031 (5 μ M) resulted in no tail current demonstrating that only I_{Kr} is present under these recording conditions.

In the recent years, notable attempts were made towards developing *in silico* biophysical models of hiPSC-CMs which reasonably reproduce the experimental AP morphology and intracellular calcium dynamics of hiPSC-CMs [27,28]. Most of these models were parameterized by averaging a large amount of *in vitro* data from multiple sources in order to cover the range of variability seen in these cells. This approach addresses the limitations of earlier models which were based on inadequate data. However,

the unresolved inconsistencies in experimental protocols used by the various sources have the potential to introduce unwarranted deviations in the hiPSC-CM electrophysiological parameter range as well as the generalizability of the baseline model. For example, blocking I_{Kr} by 33% resulted in 60% prolongation in APD_{90} in Koivumäki et al. model [29] whereas up to 59% I_{Kr} block produces mere $21.8 \pm 10\%$ APD_{90} prolongation in Kernik et al. [28]. Such large variations in model behavior could be attributed to the fact that the I_{Kr} formulation in Koivumäki model was based on adult ventricular myocyte kinetics [30] which was scaled by averaging experimental data from seven different sources, experimental conditions of which most were “not known”. The Kernik model I_{Kr} formulation was parameterized by averaging experimental data from four different sources. Moreover, none of these models include I_{KACH} , whose channels have recently been found to be present and functional in hiPSC-CMs [31]. The inclusion of I_{KACH} , allows for the investigation of the variability in the spontaneous beating frequency influenced by parasympathetic influences and/or the presence of acetylcholine which have been found to reduce the heart rate.

We implemented a genetic algorithm-based optimization method to fit the experimental I-V curves of five key currents in hiPSC-CMs to mathematical formulations from adult human atrial and sinoatrial cell models. Our aim was to utilize experimental data from a single source to maintain consistent experimental conditions and protocols as far as possible. Therefore, we utilized data acquired in our lab on the following five key currents: fast sodium current, I_{Na} ; transient outward potassium current, I_{to} ; L-type calcium current, I_{CaL} ; rapid delayed rectifier potassium, I_{Kr} ; and hyperpolarization-activated current, I_f . The Hodgkin-Huxley style characteristic equations of current density as well as activation/inactivation gating for these currents were formulated. The parameter sets of each current formulation were combined together as chromosomes and were

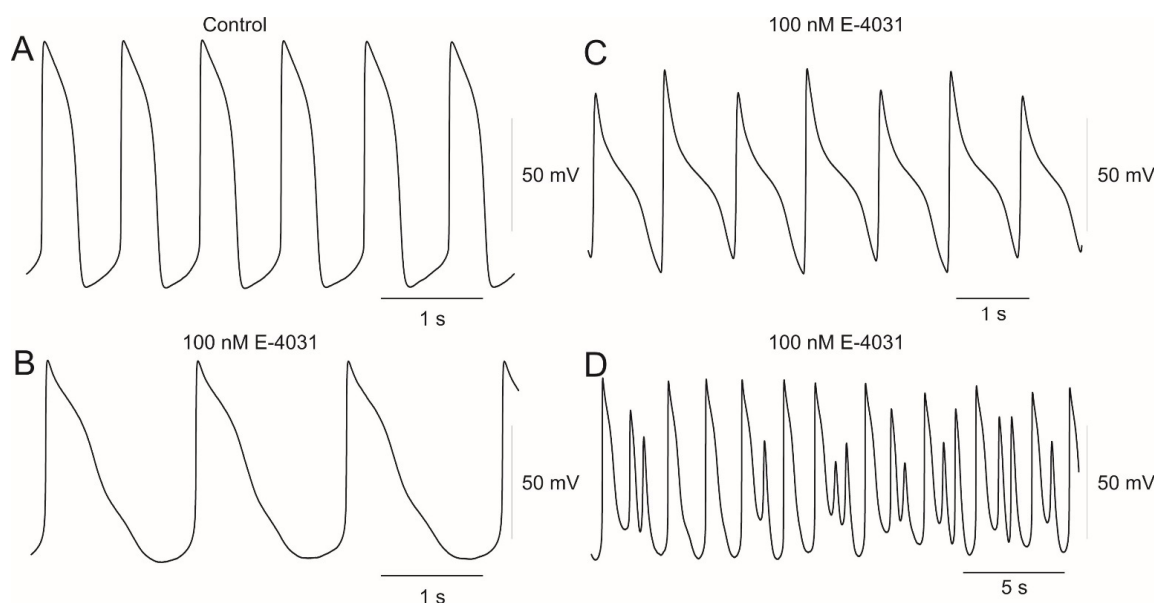


Figure 1: APs showing spontaneous activity (Panel A) and triangulation of the hiPSC myocyte AP following exposure to E-4031 (Panel B). Repolarization alternans (Panel C) and early afterdepolarizations (Panel D) were also observed following application of E-4031.

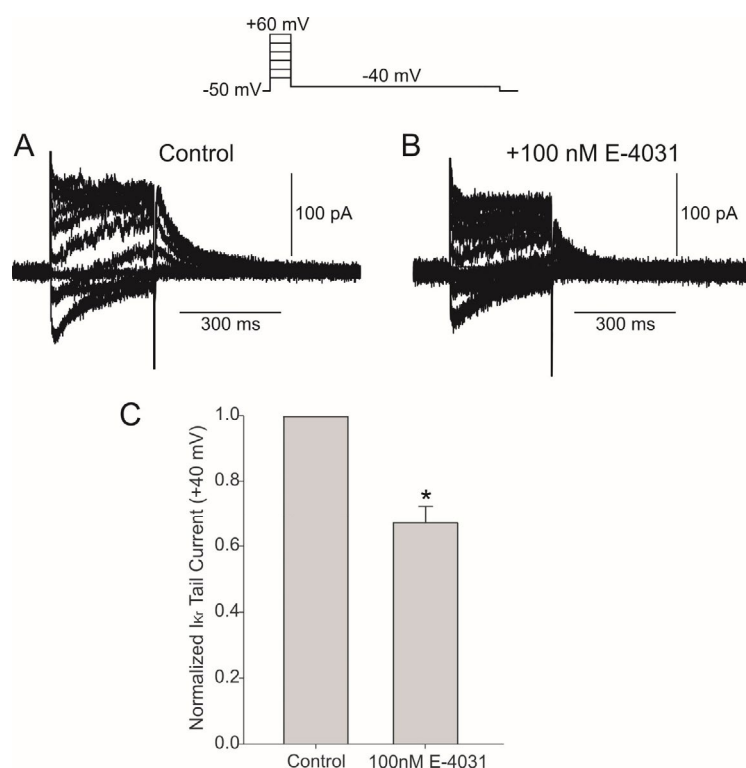


Figure 2: Representative I_{Kr} traces recorded from a hiPSC-CM in the absence (Panel A) and presence of the I_{Kr} inhibitor E-4031 (Panel B). The voltage clamp protocol is shown at the top of the figure. Summary data showing that 100 nM E-4031 decreased the size of I_{Kr} tail currents (Panel C). *significantly different compared to control.

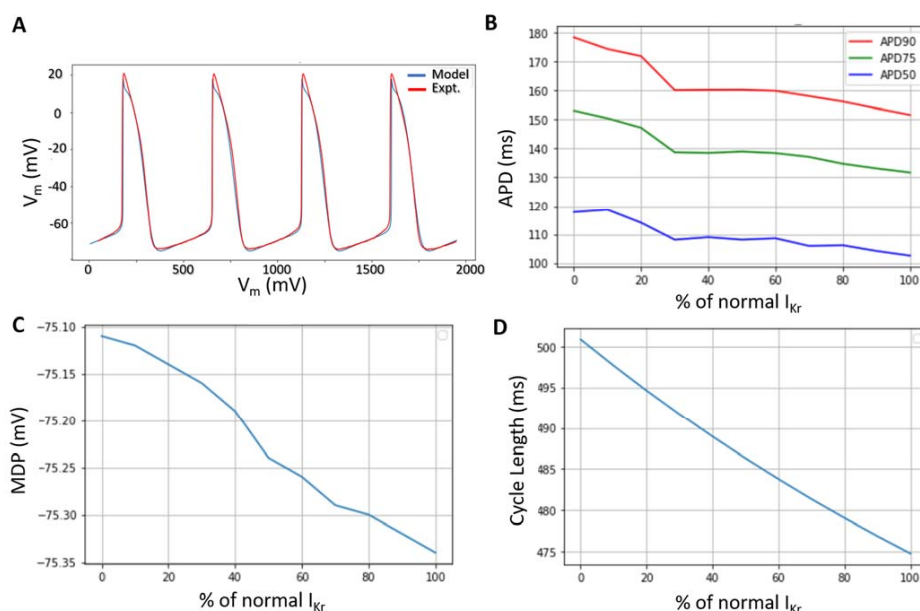


Figure 3: Computer model outcome. A) AP morphology and spontaneous triggering of APs in computer model (blue) compared to experimental data (red). B) AP prolongation at various levels of I_{Kr} blockade. C) Depolarization of MDP and D) increase in cycle length (CL) of spontaneous APs for varying levels of I_{Kr} block.

optimized heuristically by genetic algorithm over 100 generations [32]. The maximum conductances of the remaining ionic channels were then scaled based on recommendations from literature to reasonably reproduce the experimentally observed hiPSC-CM action potential morphology and automaticity. Our numerical model was able to accurately reproduce the experimentally recorded AP morphology of hiPSC-CMs as well as their automaticity (Figure 3A). We then studied the effects of varying I_{Kr} blockade in our model by scaling the maximum conductance of I_{Kr} (G_{Kr}) from 0-100%. It was observed that the APD was prolonged by approximately 15% when I_{Kr} was blocked completely (Figure 3B). The MDP was elevated slightly as the extent of I_{Kr} block was increased (Figure 3C) and the basic cycle length of spontaneous APs was monotonically increased with the extent of I_{Kr} block (Figure 3D). Our model qualitatively reproduced the depolarization of the resting membrane potential in presence of I_{Kr} block. However, it should be noted that the model being generic, did not produce the severe effects of long-term I_{Kr} block such as triangulation of AP and alternans/EADs as observed in the experiments which warrants a more systematic *in silico* investigation.

Summary and Conclusions

In hiPSC myocytes, I_{Kr} is important in determining the MDP and plays a role in controlling action potential duration. Inhibition of this current by low concentrations of E-4031 (100nM) results in depolarization of MDP, prolongation of the APD and development of EADs. These effects in hiPSC myocytes are in contrast to those seen in adult ventricular myocytes. In both guinea pig and rabbit ventricular myocytes, application of 10 μ M E-4031 resulted in about a 70ms prolongation of the action potential duration [33] and no depolarization of the membrane potential was observed. Similarly, Gintant demonstrated that 5 μ M E-4031 applied to canine midmyocardial cells caused a 100 ms prolongation in the APD [34]. These results highlight that micromolar concentrations of E-4031 produce modest changes in APD in adult myocytes whereas nanomolar concentration produce dramatic changes in hiPSC myocytes, namely depolarization of MDP, AP prolongation and EADs. The deficiency of several K^+ currents important for repolarization (such as I_{K1} and I_{Kr}) is likely responsible for the higher sensitivity of hiPSC-CMs to I_{Kr} inhibition. It is worth noting that canine ventricular myocytes exhibit depolarization of the membrane potential and EADs when exposed to combine I_{Kr} and I_{K1} blockade [35].

Safety Pharmacology and the Use of hiPSC-CM to Study I_{Kr} ?

hiPSC-CM are utilized in many applications such as models of cardiac genetic diseases [36-38]. In addition, the utilization of hiPSC-CMs for safety pharmacology is becoming more attractive as highlighted by the proposed Comprehensive In Vitro Pro-Arrhythmia Assay (CiPA) initiative [14]. CiPA aims to examine how pharmaceutical agents bound for regulatory submission to the Food and Drug Administration will affect multiple ion channels in adult cardiac tissue as well as in stem cell derived human cardiac myocytes. This new drug testing paradigm will replace the hERG channel/Purkinje fiber assay to assess potential QT prolongation of novel compounds. The use of hiPSC-CMs would seem like the ideal experimental model in that large quantities of human cardiac cells can be generated and high throughput electrophysiological analysis can be performed. Our experimental and modeling results would suggest

the hiPSC-CMs are an excellent platform for assessing cardiotoxicity as hiPSC-CMs and adult native myocytes exhibit a similar response to selective I_{Kr} blockade which may facilitate *in vitro* identification of drug-induced effects. However, since hiPSC myocytes have a low repolarization reserve compared to adult ventricular myocytes, this cell type has a greater arrhythmogenic potential due to excessive APD prolongation.

Funding Support

This study was supported by the Free and Accepted Masons of New York, Florida, Massachusetts, Connecticut, Maryland, Wisconsin, Washington, and Rhode Island (to JMC). This study was supported by National Institutes of Health (NIH) award no. 1R15HL145530-01A1 (to MD).

Conflicts of Interest

No conflicts of interests to declare.

References

1. Tse G. Mechanisms of cardiac arrhythmias. Journal of Arrhythmia. 2016 Apr 1;32(2):75-81.
2. Cordeiro JM, Callø K, Aschar-Sobbi R, Kim KH, Korogyi A, Occhipinti D, et al. Physiological roles of the transient outward current I_t . Frontiers in Bioscience. 2016 Jan 1;8:143-59.
3. Roden DM. Taking the "idio" out of "idiosyncratic": predicting torsades de pointes. Pacing and Clinical Electrophysiology. 1998 May;21(5):1029-34.
4. Dumaine R, Cordeiro JM. Comparison of K^+ currents in cardiac Purkinje cells isolated from rabbit and dog. Journal of Molecular and Cellular Cardiology. 2007 Feb 1;42(2):378-89.
5. Jost N, Virág L, Comtois P, Ördög B, Szuts V, Seprényi G, et al. Ionic mechanisms limiting cardiac repolarization reserve in humans compared to dogs. The Journal of Physiology. 2013 Sep 1;591(17):4189-206.
6. Lengyel C, Varró A, Tábori K, Papp J, Baczkó I. Combined pharmacological block of I_{Kr} and I_{Ks} increases short-term QT interval variability and provokes torsades de pointes. British Journal of Pharmacology. 2007 Aug;151(7):941-51.
7. Sanguinetti MC, Jiang C, Curran ME, Keating MT. A mechanistic link between an inherited and an acquired cardiac arrhythmia: HERG encodes the I_{Kr} potassium channel. Cell. 1995 Apr 21;81(2):299-307.
8. Sanguinetti MC, Curran ME, Spector PS, Keating MT. Spectrum of HERG K^+ -channel dysfunction in an inherited cardiac arrhythmia. Proceedings of the National Academy of Sciences. 1996 Mar 5;93(5):2208-12.
9. Roy ML, Dumaine R, Brown AM. HERG, a primary human ventricular target of the nonsedating antihistamine terfenadine. Circulation. 1996 Aug 15;94(4):817-23.
10. Di Diego JM, Belardinelli L, Antzelevitch C. Cisapride-induced transmural dispersion of repolarization and torsade de pointes in the canine left ventricular wedge preparation during epicardial stimulation. Circulation. 2003 Aug 26;108(8):1027-33.
11. Roden DM. Predicting drug-induced QT prolongation and torsades de pointes. The Journal of Physiology. 2016 May 1;594(9):2459-68.
12. Bohnen MS, Peng G, Robey SH, Terrenoire C, Iyer V, Sampson KJ, et al. Molecular pathophysiology of congenital long QT syndrome. Physiological Reviews. 2017 Jan;97(1):89-134.

13. Colatsky T, Fermini B, Gintant G, Pierson JB, Sager P, Sekino Y, et al. The comprehensive in vitro proarrhythmia assay (CiPA) initiative—update on progress. *Journal of Pharmacological and Toxicological Methods*. 2016 Sep 1;81:15-20.
14. Fermini B, Hancox JC, Abi-Gerges N, Bridgland-Taylor M, Chaudhary KW, Colatsky T, et al. A new perspective in the field of cardiac safety testing through the comprehensive in vitro proarrhythmia assay paradigm. *Journal of Biomolecular Screening*. 2016 Jan;21(1):1-1.
15. Bett GC, Kaplan AD, Lis A, Cimato TR, Tzanakakis ES, Zhou Q, et al. Electronic “expression” of the inward rectifier in cardiocytes derived from human-induced pluripotent stem cells. *Heart Rhythm*. 2013 Dec 1;10(12):1903-10.
16. Cordeiro JM, Nesterenko VV, Sicouri S, Goodrow Jr RJ, Treat JA, Desai M, et al. Identification and characterization of a transient outward K⁺ current in human induced pluripotent stem cell-derived cardiomyocytes. *Journal of Molecular and Cellular Cardiology*. 2013 Jul 1;60:36-46.
17. Qu Y, Vargas HM. Proarrhythmia risk assessment in human induced pluripotent stem cell-derived cardiomyocytes using the maestro MEA platform. *Toxicological Sciences*. 2015 Sep 1;147(1):286-95.
18. Parikh SS, Blackwell DJ, Gomez-Hurtado N, Frisk M, Wang L, Kim K, et al. Thyroid and glucocorticoid hormones promote functional T-tubule development in human-induced pluripotent stem cell-derived cardiomyocytes. *Circulation Research*. 2017 Dec 8;121(12):1323-30.
19. Zhang J, Klos M, Wilson GF, Herman AM, Lian X, Raval KK, et al. Extracellular matrix promotes highly efficient cardiac differentiation of human pluripotent stem cells: the matrix sandwich method. *Circulation Research*. 2012 Oct 12;111(9):1125-36.
20. Verkerk AO, Veerman CC, Zegers JG, Mengarelli I, Bezzina CR, Wilders R, et al. Patch-clamp recording from human induced pluripotent stem cell-derived cardiomyocytes: improving action potential characteristics through dynamic clamp. *International Journal of Molecular Sciences*. 2017 Sep;18(9):1873.
21. Calloe K, Di Diego JM, Hansen RS, Nagle SA, Treat JA, Cordeiro JM, et al. A dual potassium channel activator improves repolarization reserve and normalizes ventricular action potentials. *Biochemical Pharmacology*. 2016 May 15;108:36-46.
22. Treat JA, Goodrow RJ, Bot CT, Haedo RJ, Cordeiro JM. Pharmacological enhancement of repolarization reserve in human induced pluripotent stem cells derived cardiomyocytes. *Biochemical Pharmacology*. 2019 Nov 1;169:113608.
23. Doss MX, Di Diego JM, Goodrow RJ, Wu Y, Cordeiro JM, Nesterenko VV, et al. Maximum diastolic potential of human induced pluripotent stem cell-derived cardiomyocytes depends critically on IKr. *PLoS One*. 2012 Jul 5;7(7):e40288.
24. Gintant GA, Limberis JT, McDermott JS, Wegner CD, Cox BF. The canine Purkinje fiber: an in vitro model system for acquired long QT syndrome and drug-induced arrhythmogenesis. *Journal of Cardiovascular Pharmacology*. 2001 May 1;37(5):607-18.
25. Gintant G, Kaushik EP, Feaster T, Stoelzle-Feix S, Kanda Y, Osada T, et al. Repolarization studies using human stem cell-derived cardiomyocytes: Validation studies and best practice recommendations. *Regulatory Toxicology and Pharmacology*. 2020 Aug 19:104756.
26. Lu HR, Marien R, Saels AN, de Clerck FR. Species plays an important role in drug-induced prolongation of action potential duration and early afterdepolarizations in isolated Purkinje fibers. *Journal of Cardiovascular Electrophysiology*. 2001 Jan;12(1):93-102.
27. Paci M, Hyttinen J, Rodriguez B, Severi S. Human induced pluripotent stem cell-derived versus adult cardiomyocytes: an in silico electrophysiological study on effects of ionic current block. *British Journal of Pharmacology*. 2015 Nov;172(21):5147-60.
28. Kernik DC, Morotti S, Wu H, Garg P, Duff HJ, Kurokawa J, et al. A computational model of induced pluripotent stem-cell derived cardiomyocytes incorporating experimental variability from multiple data sources. *The Journal of Physiology*. 2019 Sep;597(17):4533-64.
29. Koivumäki JT, Naumenko N, Tuomainen T, Takalo J, Oksanen M, Puttonen KA, et al. Structural immaturity of human iPSC-derived cardiomyocytes: in silico investigation of effects on function and disease modeling. *Frontiers in physiology*. 2018 Feb 7;9:80.
30. ten Tusscher KH, Noble D, Noble PJ, Panfilov AV. A model for human ventricular tissue. *American Journal of Physiology-Heart and Circulatory Physiology*. 2004 Apr;286(4):H1573-89.
31. Zhao Z, Lan H, El-Battrawy I, Li X, Buljubasic F, Sattler K, et al. Ion channel expression and characterization in human induced pluripotent stem cell-derived cardiomyocytes. *Stem Cells International*. 2018 Oct;2018.
32. Akwaboah AD, Yamlome P, Treat JA, Cordeiro JM, Deo M. Genetic Algorithm For Fitting Cardiac Cell Biophysical Model Formulations. In 2020 42nd Annual International Conference of the IEEE Engineering in Medicine & Biology Society (EMBC) 2020 Jul 20 (pp. 2463-2466). IEEE.
33. Lu Z, Kamiya K, Opthof T, Yasui K, Kodama I. Density and kinetics of I Kr and I Ks in guinea pig and rabbit ventricular myocytes explain different efficacy of I Ks blockade at high heart rate in guinea pig and rabbit: implications for arrhythmogenesis in humans. *Circulation*. 2001 Aug 21;104(8):951-6.
34. Gintant GA. Two components of delayed rectifier current in canine atrium and ventricle: does IKs play a role in the reverse rate dependence of class III agents?. *Circulation Research*. 1996 Jan 1;78(1):26-37.
35. Biliczki P, Virág L, Iost N, Papp JG, Varró A. Interaction of different potassium channels in cardiac repolarization in dog ventricular preparations: role of repolarization reserve. *British Journal of Pharmacology*. 2002 Oct;137(3):361-8.
36. Itzhaki I, Maizels L, Huber I, Zwi-Dantsis L, Caspi O, Winterstern A, et al. Modelling the long QT syndrome with induced pluripotent stem cells. *Nature*. 2011 Mar;471(7337):225-9.
37. Terrenoire C, Wang K, Chan Tung KW, Chung WK, Pass RH, Lu JT, et al. Induced pluripotent stem cells used to reveal drug actions in a long QT syndrome family with complex genetics. *Journal of General Physiology*. 2013 Jan 1;141(1):61-72.
38. Selga E, Sendfeld F, Martinez-Moreno R, Medine CN, Tura-Ceide O, Wilmut I, et al. Sodium channel current loss of function in induced pluripotent stem cell-derived cardiomyocytes from a Brugada syndrome patient. *Journal of Molecular and Cellular Cardiology*. 2018 Jan 1;114:10-9.